Original Article

Differentiation of localized pneumonic-type lung adenocarcinoma from localized pulmonary inflammatory lesion based on clinical data and multi-slice spiral computed tomography imaging features

Yisi Xiang[1#], Min Zhang[1#], Weiyan Zhao[1], Hengfeng Shi[2]^

[1]Department of Radiology, Xuancheng People's Hospital of Anhui Province, Xuancheng, China; [2]Department of Radiology, Anqing Municipal Hospital of Anhui Province, Anqing, China

Contributions: (I) Conception and design: Y Xiang, M Zhang, H Shi; (II) Administrative support: Y Xiang, M Zhang, H Shi; (III) Provision of study materials or patients: All authors; (IV) Collection and assembly of data: All authors; (V) Data analysis and interpretation: All authors; (VI) Manuscript writing: All authors; (VII) Final approval of manuscript: All authors.

[#]These authors contributed equally to this work.

Correspondence to: Hengfeng Shi. Department of Radiology, Anqing Municipal Hospital of Anhui Province, No. 87, Tianzhushan Road, Anqing, 246000, China. Email: shihengfeng@163.com.

Background: Localized pneumonic-type lung adenocarcinoma (L-PLADC) is a special type of lung adenocarcinoma, which mimicking localized pulmonary inflammatory lesion (L-PIL), and many delayed diagnoses of L-PLADC have been identified due to insufficient clinical understanding or the lack of knowledge regarding the radiological findings. Multi-slice spiral computed tomography (MSCT) not only observes the fine structure of the lesion clearly, but also can evaluate the lesion and its surrounding tissues more intuitively, stereoscopically, and accurately using a variety of reconstruction techniques. The present study aimed to investigate the diagnostic value of clinical data and MSCT imaging features in differentiating L-PLADC from L-PIL.

Methods: The clinical data and chest MSCT imaging features of 71 patients with L-PLADC and 70 patients with L-PIL were retrospectively analyzed. Seventy-one patients with L-PLADC underwent surgical resection or puncture and were confirmed as having invasive adenocarcinoma by pathology. Seventy patients with L-PIL were confirmed by clinical anti-inflammatory treatment or by puncture and surgery. The Chi-square and Mann-Whitney U tests were used to analyze the clinical data and MSCT imaging features of the included patients. Variables with $P<0.05$ in the univariate analysis were included in the multivariate logistic regression analysis to determine the independent risk factors for the diagnosis of L-PLADC.

Results: The clinical data analysis showed that multivariate logistic regression analysis showed that irregular air bronchogram [odds ratio (OR) =15.946; $P<0.001$], ground-glass opacity (GGO) component (OR =12.369; $P<0.001$), pleural traction (OR =10.982; $P<0.001$), necrosis (OR =0.078; $P<0.001$), adjacent bronchial wall thickening (OR =0.017; $P<0.001$), pleural thickening (OR =0.074; $P<0.001$), and respiratory symptoms were independent risk factors for the diagnosis of L-PLADC [OR =0.117; the area under the curve (AUC), sensitivity, specificity, and accuracy values were 0.989, 97.2%, 94.3%, and 95.7%, respectively].

Conclusions: L-PLADC and L-PIL exhibit different clinical and MSCT imaging features. Determining these characteristics is conducive to the early diagnosis and clinical treatment of L-PLADC.

Keywords: Pneumonic lung adenocarcinoma; inflammation; multi-slice spiral computed tomography (MSCT)

^ ORCID: 0000-0002-8980-1335.

Submitted Oct 13, 2022. Accepted for publication Dec 05, 2022. Published online Dec 19, 2022.
doi: 10.21037/tcr-22-2525
View this article at: https://dx.doi.org/10.21037/tcr-22-2525

Introduction

Clinically, primary lung adenocarcinoma with patchy, large patchy consolidation, or ground-glass shadow on chest computed tomography (CT) images is usually called pneumonic-type lung adenocarcinoma (PLADC) (1,2). Previous studies (3-8) have divided PLADC into localized pneumonic-type lung adenocarcinoma (L-PLADC) and diffuse lung adenocarcinoma. L-PLADC is defined as a PLADC with a single lobe and isolated localized lesions that make up less than 50% of the lobe area. L-PLADC is very similar to a localized pulmonary inflammatory lesion (L-PIL) and is easily misdiagnosed. Sputum-exfoliated cells, brush cytology, or fiberoptic bronchoscopy are relatively difficult to diagnose this type of lung cancer. Some patients cannot be diagnosed immediately, even by percutaneous lung biopsy, In addition, due to the overlap of clinical data and MSCT imaging signs, the initial diagnosis is difficult. Some patients began to suspect tumor and were confirmed by surgery or biopsy after long and repeated follow-up, so that most L-PLADC patients are delayed in diagnosis, which is largely due to insufficient understanding of the importance of combining clinical data with imaging features. Multi-slice spiral computed tomography (MSCT) not only observes the fine structure of the lesion clearly, but also can evaluate the lesion and its surrounding tissues more intuitively, stereoscopically, and accurately using a variety of reconstruction techniques. The present study aimed to evaluate the diagnostic value of clinical data and MSCT features in differentiating L-PLADC from focal L-PIL. We present the following article in accordance with the STARD reporting checklist (available at https://tcr.amegroups.com/article/view/10.21037/tcr-22-2525/rc).

Highlight box

Key findings

- Our results demonstrated that L-PLADC has certain clinical and MSCT imaging features. Patients with focal pulmonary consolidation with irregular bronchial inflation, GGO composition, pleural traction, no necrosis, adjacent bronchial wall thickening, pleural thickening, and respiratory symptoms should be suspected of L-PLADC.

What is known and what is new?

- L-PLADC is a special type of lung adenocarcinoma,which mimicking L-PIL,and many delayed diagnoses of L-PLADC have been identified due to insufficient clinical understanding or the lack of knowledge regarding the radiological findings.
- L-PLADC and L-PIL exhibit different clinical and MSCT imaging features.

What is the implication, and what should change now?

- An adequate understanding of these different clinical and MSCT imaging features can contribute to the early diagnosis of L-PLADC and the subsequent therapeutic strategy.

Methods

Data source

L-PLADC was identified using the following diagnostic criteria via MSCT: (I) unilobar pulmonary consolidation lesions, which could not be divided into round or oval soft tissue nodules or masses; (II) isolated and localized lesions with a maximum axial image making up less than half of the lobe area; (III) surgical pathology-confirmed lung adenocarcinoma; (IV) patients with primary lung adenocarcinoma. L-PIL was identified using the following diagnostic criteria via MSCT: (I) single lobe lung consolidation lesion, with the maximum transverse axis image constituting less than half of the lung lobe area; (II) patients with inflammatory lesions confirmed by surgery, puncture pathology, or clinical treatment. Hospitalized cases from Xuancheng People's Hospital and Anqing Municipal Hospital in Anhui from January 2020 to June 2022 were collected. These patients with L-PLADC and L-PIL fulfilled the following inclusion criteria: all of the included patients underwent chest CT and enhanced scanning. Patients who received anti-tumor or anti-inflammatory treatment prior to the first chest CT scan were excluded. The study was conducted in accordance with the Declaration of Helsinki (as revised in 2013). The study was approved by ethics committee of Xuancheng People's

Hospital (No. 2022-LW007-01). Informed consent was taken from all the patients. Anqing Municipal Hospital in Anhui was informed and agreed with the study.

MSCT examination method

Chest CT scanning was carried out using an American General Electric Company GE 64-slice CT scanner. First, a CT scan from the apex of the lung to the bottom of the lung was performed in the supine position. The scanning parameters were as follows: tube voltage, 120 kVp; tube current, 160–250 mA; scanning layer thickness, 5 mm; and layer spacing, 5 mm. The contrast agent injection protocol was as follows: non-ionic iodinated contrast agent (iohexol 300 mg iodine/mL, iodixanol 320 mg iodine/mL) was injected through the contralateral forearm vein using a high-pressure syringe at a flow rate of 3.0 mL/s and a dose of 1.2 mL/kg (total volume: 60–100 mL). The acquisition time of the arterial and delayed phases was scanned at 30 and 60 seconds after the injection of the contrast agent, respectively, and the reconstructed 1 mm image was analyzed.

Evaluation method

Two chest imaging radiologists with more than 10 years of work experience read the images on picture archiving and communication systems (PACS) using the double-blind method, and an agreement was reached in cases where the opinions of the radiologists were inconsistent. A careful analysis of the CT features of the lesion was conducted as follows:

(I) Lesion location: left upper and lower lobe; and right upper, middle, and lower lobe.
(II) Size: the lung window was measured as the longest diameter of the largest cross-section of the lesion.
(III) Boundaries: clear or fuzzy.
(IV) Internal characteristics: Bronchial inflation sign (branch or tubular inflatable bronchus in the lesion, smooth inner wall, unobstructed lumen, and natural course), irregular bronchial inflation sign (bronchiectasis, distortion or rigidity, stenosis or truncation in the lesion), air-containing cavity (cystic air-containing cavity in the nodule, which is not connected with the bronchus), ground-glass-like shadow (macroscopic observation of the lung window is higher than the background lung tissue without masking the bronchial vascular bundle, and the boundary with normal lung tissue is clear), necrosis (low density in the lesion without enhancement), and calcification.
(V) External characteristics: satellite lesions (≤3 cm from the consolidation around the lesion), halo sign (ground-glass shadow with an unclear boundary around the consolidation), thickening of the adjacent bronchial wall (the thickness of the bronchial wall is ≥ twice than that of the adjacent normal bronchial wall), thickening of the adjacent interlobular septum, pleural traction (one or more linear shadows between the surface of the lesion and the pleura, accompanied by pleural shrinkage), close to the pleura, and adjacent pleural thickening.
(VI) Other signs: lymph node lesions (hilar or mediastinal enlarged lymph nodes, short axis diameter >1 cm) and pleural effusion.

Statistical method

Statistical analysis was performed using SPSS 23.0 (IBM SPSS Inc., Chicago, IL, USA). The Youden's index (YI) (YI = sensitivity + specificity − 1) of age was calculated by receiver operating characteristic (ROC) curve analysis, and the optimal thresholds for L-PLADC and L-PIL were determined with a maximum value. Measurement data conforming to a normal distribution and homogeneity of variance were expressed as $\bar{x}\pm s$ and compared using the independent sample t-test. Skew distributions or heteroscedasticity were expressed as M (Q1, Q3) and compared using the Mann-Whitney U test. Count data were expressed as numbers and percentages using the chi-square test or Fisher exact probability method.

Multivariate logistic regression analysis on the clinical data and MSCT features with significant differences between groups was performed to determine the independent factors for the diagnosis of L-PLADC, and a predictive model was established to evaluate its diagnostic performance using the area under the curve (AUC), sensitivity, specificity, and accuracy.

Results

Initially, 78 patients with L-PLADC and 85 patients with L-PIL were included, among whom 22 patients were excluded because they had received anti-tumor or anti-inflammatory treatment prior to the first chest CT scan. Finally, 71 patients with L-PLADC and 70 patients with L-PIL were included for analysis. The patient selection

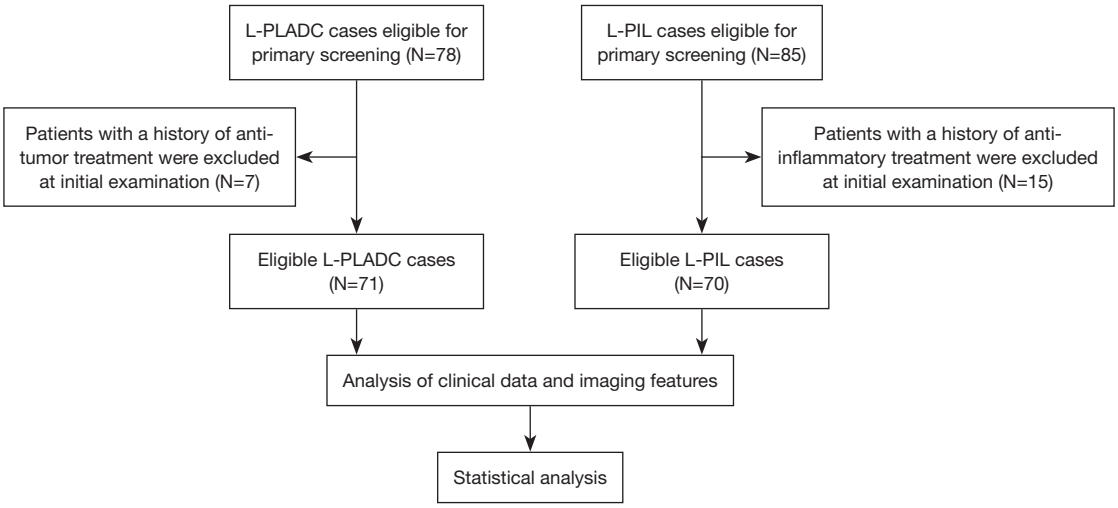

Figure 1 Study flow chart. L-PLADC, localized pneumonic-type lung adenocarcinoma; L-PIL, localized pulmonary inflammatory lesions.

process is shown in *Figure 1*.

Seventy-one patients with L-PLADC underwent surgical resection or puncture and were confirmed as having invasive adenocarcinoma by pathology. Among them, 42 cases (59.15%) were mainly acinar type, 16 cases (22.54%) were mainly adherent type, eight cases (11.27%) were mainly papillary type, two cases (2.82%) were mainly micropapillary type, and two cases (2.82%) were histological subtypes of mucinous adenocarcinoma. One case (1.41%) showed acinar type and micropapillary type, each accounting for about 50%.

Among the 70 patients with L-PIL, 29 cases (38.57%) were confirmed by clinical anti-inflammatory treatment, and 23 cases (32.86%) were confirmed by puncture and surgery. Moreover, there were 15 cases (21.43%) of surgically confirmed pulmonary tuberculosis and three cases (4.29%) of surgically confirmed fungus.

Comparison of the clinical data between L-PLADC and L-PIL (see Table 1)

The L-PLADC patients were between 43 and 83 years old, with an average [± interquartile range (IQR)] of 66.0±13.0 years, while the L-PIL patients were 37–86 years old, with an average (± IQR) of 58.5±17.3 years. The L-PLADC patients were older than those with L-PIL (P<0.05). The optimal age threshold for distinguishing L-PLADC from L-PIL was 63.5 years, with an AUC of 0.600, a sensitivity of 63.4%, and a specificity of 58.6%. L-PLADC was more common than L-PIL in patients aged ≥64 years old, females, and those with no respiratory symptoms (P<0.05).

Comparison of the CT features between the two groups of patients (see Table 2)

The CT features of the two groups were summarized. The longest diameter of the lesions in the L-PLADC group was 2.00 (1.60, 2.50) cm, while that in the L-PIL group was 2.25 (1.60, 4.33) cm. An irregular air bronchogram, ground-glass opacity (GGO) component, and pleural traction were more common in the L-PLADC group (*Figures 2,3*), while an air bronchogram, necrosis, calcification, satellite lesions, adjacent bronchial wall thickening, adjacent interlobular septal thickening, adjacent pleural thickening, and pleural effusion were more common in the L-PIL group (P<0.05) (*Figures 4,5*).

Multivariate analysis of the clinical data and MSCT features between the two groups (see Table 3)

The statistically significant factors in the univariate analysis were included in the multivariate logistic regression analysis, which showed that irregular air bronchogram [odds ratio (OR) =15.946; P<0.001], GGO component (OR =12.369; P<0.001), pleural traction (OR =10.982; P<0.001), necrosis (OR =0.078; P<0.001), adjacent bronchial wall thickening (OR =0.017; P<0.001), adjacent pleural thickening (OR =0.074; P<0.001), and respiratory symptoms (OR =0.117; P<0.001) were independent risk factors for predicting L-PLADC. The AUC, sensitivity, specificity, and accuracy

Table 1 Comparison of the clinical features between focal inflammatory lung adenocarcinoma and pulmonary focal inflammatory lesions

Characteristics	L-PLADC patients (n=71)	L-PIL patients (n=70)	P value
Age (years), n (%)			0.009
<64	26 (36.62%)	41 (58.57%)	
≥64	45 (63.38%)	29 (41.43%)	
Gender, n (%)			0.014
Male	24 (33.80%)	38 (54.29%)	
Female	47 (66.20%)	32 (45.71%)	
Smoking history, n (%)			0.179
Non-smokers	61 (85.92%)	54 (77.14%)	
Smokers	10 (14.08%)	16 (22.86%)	
Respiratory tract symptoms, n (%)			<0.001
Symptomatic	16 (22.54%)	42 (60.00%)	
Fever	1	4	
Cough	12	33	
Expectoration	10	27	
Bloody sputum	0	5	
Hemoptysis	1	4	
Chest pain	3	11	
No symptoms	55 (77.46%)	28 (40.00%)	
Increased white blood cell count, n (%)	16 (22.54%)	9 (12.86%)	0.132

L-PLADC, localized pneumonic-type lung adenocarcinoma; L-PIL, localized pulmonary inflammatory lesion.

values of the logistic model were 0.989, 97.2%, 94.3%, and 95.7%, respectively.

Follow-up results

Twenty-two patients with L-PLADC were followed up, among whom seven had no change during the follow-up, while the remaining 15 lesions had progressed (including increased density, ground-glass density shadow, and air bronchogram disappeared), and the progress was obvious. The actual component increased significantly and the range also increased (*Figure 3*). The average follow-up time was 8 months (range: 19 days–32 months). Twenty-nine patients with L-PIL were followed up for an average of 2 months (range: 7 days–12 months).

Discussion

L-PLADC is very similar to L-PIL, and insufficient clinical understanding may lead to misdiagnosis or delayed diagnosis. In this study, we compared the clinical data and MSCT imaging features between L-PLADC and L-PIL, and established a predictive model through multivariate regression analysis to help distinguish the two conditions and improve the diagnostic expertise of radiologists for L-PLADC.

In terms of clinical characteristics, our results suggested that, compared to L-PIL, L-PLADC was more common in elderly women and more likely to exhibit non-respiratory symptoms. We found that, unlike L-PIL, in which most patients experience respiratory symptoms, more than 50% of L-PLADC patients have no respiratory symptoms, which is consistent with the literature (7,8). Numerous researchers have shown that LADC is more likely to be associated with non-smoking women (9,10). It should be emphasized that the number of cases of L-PLADC and L-PIL in this study is the same, which does not mean that the incidence rate of L-PLADC and L-PIL is similar. The reasons are

Table 2 Comparison of the CT features between focal inflammatory lung adenocarcinoma and focal pulmonary inflammatory lesions

CT feature	L-PLADC patients (n=71)	L-PIL patients (n=70)	P value
Position, n (%)			0.077[a]
Upper lobe	44 (61.97%)	33 (47.14%)	
Right upper lobe	19	18	
Left upper lobe	25	15	
Middle and lower lobe	27 (38.03%)	37 (52.86%)	
Right middle lobe	9	7	
Right lower lobe	5	17	
Left lower lobe	13	13	
Boundary, n (%)			0.061[a]
Clear boundary	60 (84.51%)	50 (72.43%)	
Fuzzy boundary	11 (15.49%)	20 (28.57%)	
Size, M (Q1, Q3)	2.00 (1.60, 2.50)	2.25 (1.60, 4.33)	0.079
Internal CT features, n (%)			
Air bronchogram	11 (15.49%)	40 (57.14%)	<0.001[a]
Irregular bronchial inflation sign	56 (78.87%)	8 (11.43%)	<0.001[a]
Pneumatic space	12 (16.90%)	9 (12.86%)	0.500[a]
GGO	52 (73.24%)	4 (5.71%)	<0.001[a]
Necrosis	4 (5.63%)	49 (70.00%)	<0.001[a]
Calcification	4 (5.63%)	15 (21.43%)	0.006
Garment tag, n (%)			
Satellite focal	1 (1.41%)	13 (18.57%)	0.001
The halo sign	2 (2.82%)	7 (10.00%)	0.161*
Adjacent bronchial wall thickening	1 (1.41%)	37 (52.86%)	< 0.001[a]
Adjacent interlobular septum thickening	4 (5.63%)	17 (24.29%)	0.002[a]
Pleural traction	56 (78.87%)	11 (15.71%)	<0.001[a]
Close to the pleura	14 (19.72%)	52 (74.29%)	<0.001[a]
Adjacent pleural thickening	20 (28.17%)	48 (68.57%)	<0.001[a]
Other findings, n (%)			
Mediastinal and hilar lymphadenopathy	10 (14.08%)	14 (20.00%)	0.350[a]
Hydrothorax	2 (2.82%)	11 (15.71%)	0.008

*, 1≤ T <5, there were two lattice theory frequencies less than 5; [a], Chi-squared test; P value using the corrected value. GGO, ground-glass opacity.

as follows: (I) the sample size is limited, and there is no big data of multi center research; (2) the data collection in this group strictly followed the inclusion criteria of all patients receiving chest CT and enhanced scanning. Most L-PIL patients who are more typical due to clinical symptoms and conventional images (such as X-ray and chest CT) were excluded, and even only a few patients who are difficult to diagnose were assisted by chest enhanced examination. To

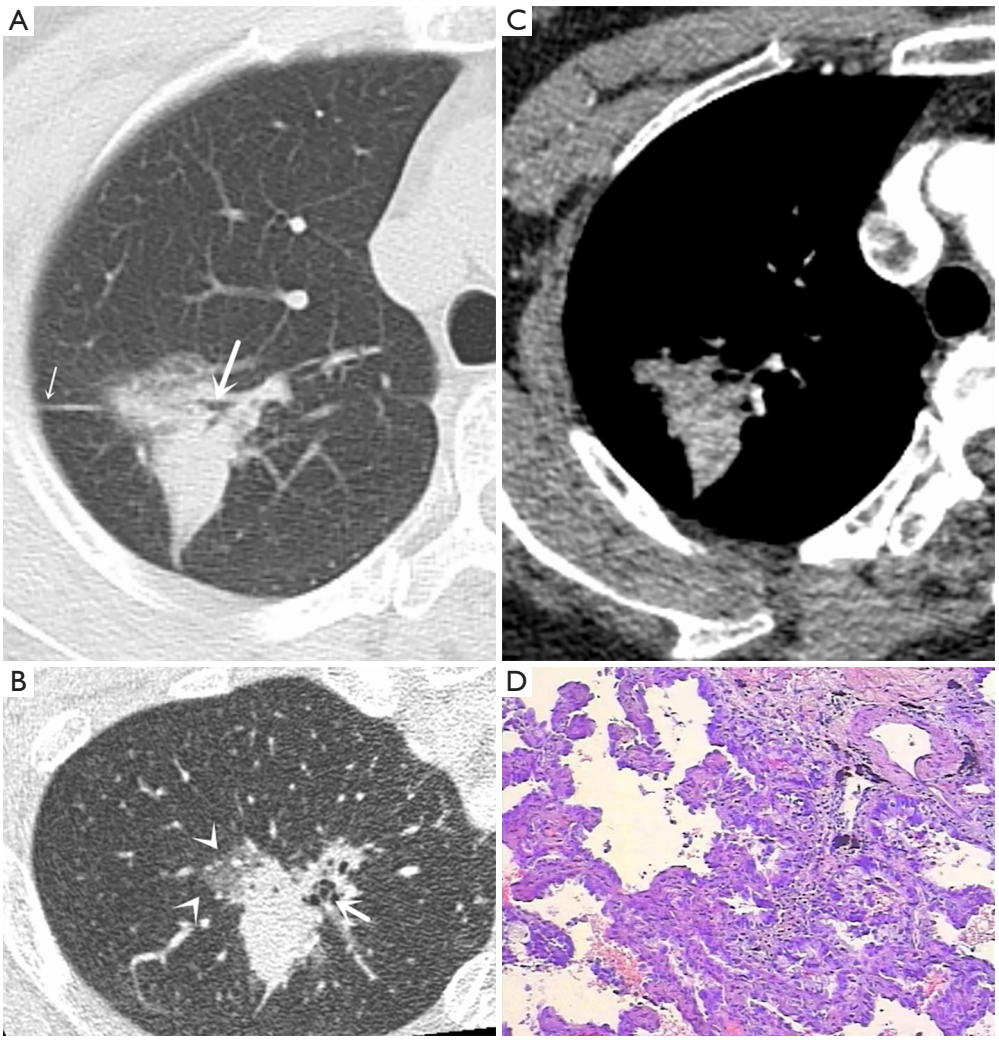

Figure 2 Female, 74 years old, with repeated dizziness for more than 1 month, no respiratory symptoms. (A,B) Lung window right upper lobe consolidation, irregular bronchiectasis (thick arrow), GGO (arrowheads), and pleural traction (thin arrow). (C) After enhancement (arterial phase), the solid components were homogeneously enhanced without necrosis. (D) Pathology: invasive adenocarcinoma (HE staining, ×200). GGO, ground-glass opacity; HE, hematoxylin and eosin.

some extent, the number of L-PIL cases in this group may be greatly reduced. However, L-PLADC patients do not have the above situation. Most L-PLADC patients need to receive chest CT and enhanced scanning before the pathological diagnosis.

As for the MSCT manifestations, the internal details and external features of the lesions can be better displayed by multiplanar reconstruction. The present study found that irregular bronchial inflation sign, GGO composition, and pleural traction indicated L-PLADC, while inflatable bronchial sign, necrosis, calcification, satellite lesions, adjacent bronchial wall, adjacent interlobular septal thickening, close to the pleura, adjacent pleural thickening, and pleural effusion suggested L-PIL.

An increasing number of people (1,7,11-13) believe that pneumonia-type lung cancer and lung inflammatory lesions bronchial inflation sign is not completely consistent. Compared with the common branch or tubular inflatable bronchial sign in inflammatory lesions, the inner bronchus is unobstructed; natural; has a smooth inner wall; rarely exhibits expansion, stenosis, or stiffness changes; shows pneumonia-type lung cancer inflatable bronchiectasis, stiffness, and uneven thickness; and can be manifested as dead branches, honeycomb sign, false cavity sign, and other

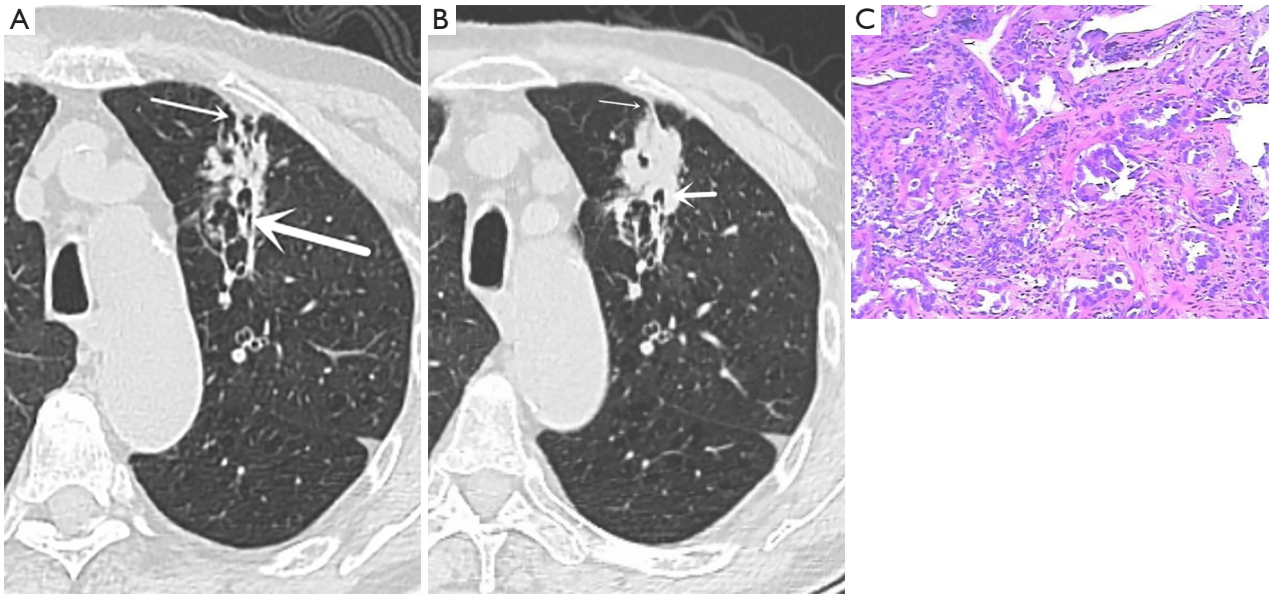

Figure 3 Male, 83 years old, dizziness and discomfort for a week, no smoking history. (A) Irregular air bronchogram (thick arrow) and pleural traction (thin arrow). The patient was misdiagnosed with chronic inflammatory lesions, and no further examination was conducted. (B) After 3 months, lesion consolidation and nodule formation were obvious, and there was bronchial truncation or disappearing (thick arrow) and pleural traction line thickening (thin arrow). (C) Pathology: invasive adenocarcinoma (HE staining, ×200). HE, hematoxylin and eosin.

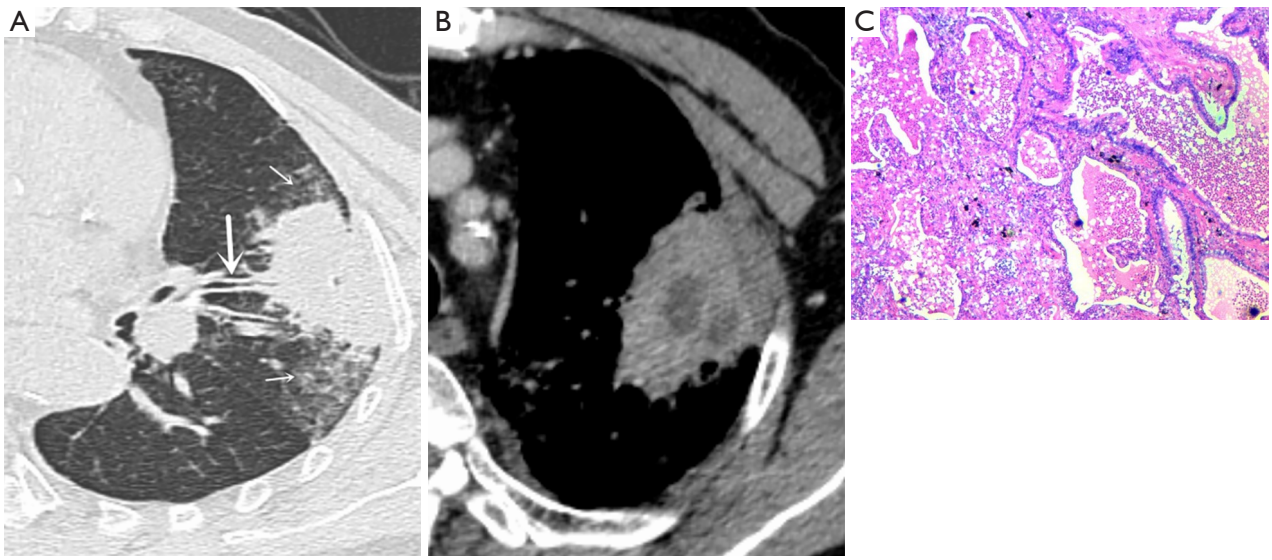

Figure 4 Male, 75 years old, coughing for more than 3 months, white blood cell count 13.61×10^9/L, lung window. (A) Axial CT showed left upper lobe localized consolidation, unclear boundary, adjacent bronchial wall thickening (thick arrow), surrounding lobular septal thickening (thin arrow), and close to the pleura with adjacent pleural thickening. (B) An enhanced scan showed no enhanced necrosis in the lesion. The patient was misdiagnosed with a tumor. (C) Surgical pathology: chronic inflammation with abscess, organization (HE staining, ×200). HE, hematoxylin and eosin.

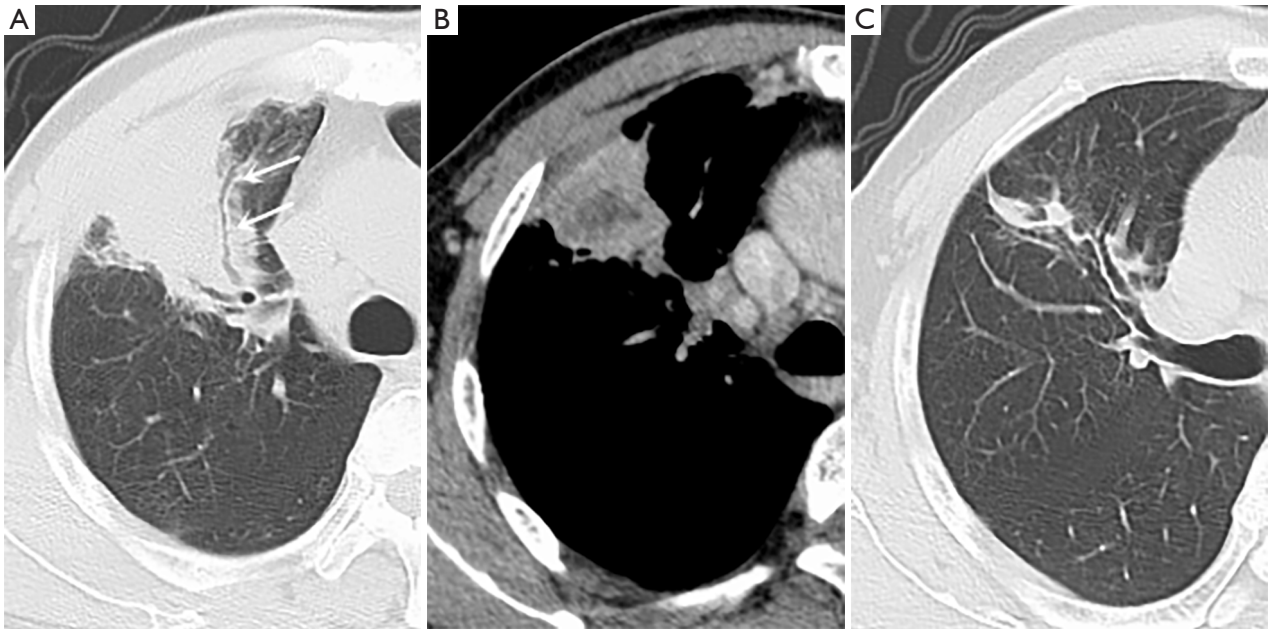

Figure 5 Male, 52 years old, cough, expectoration more than 1 month with blood in sputum for 1 week; white blood cell count was normal. (A) Right upper lobe consolidation with air bronchogram (thin arrow), smooth inner wall and walking naturally, lesions close to the pleura, and pleural thickening. (B) Enhanced scanning showed no enhanced necrotic area in the lesion. (C) Sputum culture and bronchoscopy lavage night NGS showed Klebsiella pneumonia. Clinical anti-infection treatment was administered, and re-examination after 3 months showed that the lesions were significantly absorbed.

Table 3 Independent factors for differentiating focal inflammatory lung adenocarcinoma from focal inflammatory lung lesions by multivariate logistic regression

Factors	Coefficient	Standard error	Wald X^2 value	P value	OR value	95% CI
Respiratory tract symptoms	–2.150	1.054	4.160	0.041	0.117	0.015, 0.919
Irregular bronchus inflatable sign	2.769	0.958	8.347	0.004	15.946	2.437, 104.356
Grinding glass composition	2.515	1.029	5.979	0.014	12.369	1.647, 92.883
Necrosis	–2.550	0.968	6.937	0.008	0.078	0.012, 0.521
Adjacent bronchial wall thickening	–4.086	1.819	5.048	0.025	0.017	0.000, 0.594
Pleural traction	2.396	0.960	6.231	0.013	10.982	1.673, 72.078
Adjacent pleural thickening	–2.605	0.981	7.050	0.008	0.074	0.011, 0.506
Constant	0.047	0.992	0.002	–	–	–

OR, odds ratio; CI, confidence interval.

signs. Also, due to fibrous proliferative reaction or tumor invasion, the inflatable bronchus is gradually truncated or disappears with further progression of the tumor, which is consistent with the cases of L-PLADC in the present cohort.

In this study, GGO with a clear boundary was indicative of L-PLADC. It is worth noting that GGO needs to be carefully distinguished from a halo sign, which refers to the consolidation of the surrounding boundary that is not clear ground-glass density, which is more common in inflammatory lesions (5,8,13). Some studies have shown (11,14-18) that the pathological subtypes of different

subtypes of invasive adenocarcinoma determine the density of CT, and GGO components are pathologically more common in the adherent growth, acinar, or papillary types (especially the adherent growth type).

Tumor cells grow along the alveolar wall but do not completely fill the alveolar space to form GGO imaging features. We found that the above three pathological subtypes (adherent growth, acinar, or papillary types) were more common in this group of L-PLADC pathological results, which may be an important reason for the high incidence of GGO components in this group of L-PLADC patients. Another important external sign common in L-PLADC is pleural traction, which may be related to tumor cell infiltration along the subpleural stroma or tumor contraction (19).

Our results also showed that necrosis is more common in inflammatory lesions, which is consistent with the findings of previous studies (3,8). Inflammatory necrosis is related to the inflammatory response caused by microbial infection. Inflammatory injury usually occurs earlier in the alveolar space filled with inflammatory fragments. The necrotic tissue is manifested as a low-density non-enhanced area in the center of the lesion on CT enhancement. Lung cancer has the characteristics of 'continuous angiogenesis'. Early tumor neovascularization carries nutrients and oxygen to tumor cells so that they have sufficient survival supply and are not prone to early necrosis. Tumor necrosis is caused by chronic ischemic injury or hypoxia, which is usually common in larger tumors (20). It is not difficult to understand that L-PLADC is characterized by patchy distribution due to its limited cumulative range, and does not form nodules and masses. The blood supply may be easier to meet the demand and central necrosis is relatively rare.

In addition, the findings of this study suggested that calcification, satellite lesions, and thickening of the adjacent bronchial wall and interlobular septum were more common in inflammatory lesions, which may be related to the diffusion of inflammation along the adjacent alveoli, bronchi, and mesenchyme. In contrast to the literature (3), the proportion of calcification and satellite lesions in this group was slightly higher, as was the proportion of pulmonary tuberculosis cases, which may be related to the relatively high incidence of calcification and surrounding satellite lesions in tuberculosis. Similarly, pleural thickening and pleural effusion were also highly indicative of inflammatory lesions. This may be attributable to the fact that inflammatory alveolar exudates are easy to spread under the pleura, resulting in pleurisy and even pleural effusion.

Multivariate analysis in this study showed that irregular air bronchogram, GGO component, pleural traction, no necrosis, adjacent bronchial wall thickening, pleural thickening, and respiratory symptoms were the most important independent factors for the diagnosis of L-PLADC. Familiarity with these differential features will help to accurately diagnose L-PLADC and reduce the unnecessary surgical resection rate of L-PIL.

We also observed that follow-up CT comparison might help to characterize the lesion, focusing on changes in lesion range, density, internal structure, and surrounding features. Furthermore, an absorbed lesion indicates that the possibility of pulmonary inflammation is greater. The 29 patients in the L-PIL group were confirmed to have inflammatory lesions after clinical anti-inflammatory treatment. In 15 patients with L-PLADC, the lesion progressed during CT follow-up. The tumor showed some morphological and density changes over time, such as increased density, ground-glass density shadows, solid components, and air-filled bronchus truncation or disappearance. In patients with significant progress, the actual components increased, the range increased, and even nodules or masses were formed. If the lesion does not change, a comprehensive analysis based on the above clinical and imaging features, as well as additional examinations such as biopsy, are usually required to determine the next treatment option.

This study had some limitations that should be noted. Firstly, this is a single center study with relatively limited sample size and no cooperation with other external centers, lacking external validation samples. Also, based on the high proportion of invasive adenocarcinomas in pneumonia-type lung cancer, this study only included adenocarcinoma, and other histological types were excluded.

Conclusions

In summary, as a special manifestation, L-PLADC is very similar to L-PIL. In the past, insufficient understanding and distinction between these two conditions often caused misdiagnosis or delayed diagnosis. Our results demonstrated that L-PLADC has certain clinical and MSCT imaging features. Patients with focal pulmonary consolidation with irregular bronchial inflation, GGO composition, pleural traction, no necrosis, adjacent bronchial wall thickening, pleural thickening, and respiratory symptoms should be suspected of L-PLADC. Familiarity with these features

is helpful for the early diagnosis and clinical treatment of L-PLADC.

Acknowledgments

Funding: This work was financially supported by Research Foundation of Wu Jieping Medical (No. 320.6750.2020-08-10).

Footnote

Reporting Checklist: The authors have completed the STARD reporting checklist. Available at https://tcr.amegroups.com/article/view/10.21037/tcr-22-2525/rc

Data Sharing Statement: Available at https://tcr.amegroups.com/article/view/10.21037/tcr-22-2525/dss

Conflicts of Interest: All authors have completed the ICMJE uniform disclosure form (available at https://tcr.amegroups.com/article/view/10.21037/tcr-22-2525/coif). The authors have no conflicts of interest to declare.

Ethical Statement: The authors are accountable for all aspects of the work in ensuring that questions related to the accuracy or integrity of any part of the work are appropriately investigated and resolved. The study was conducted in accordance with the Declaration of Helsinki (as revised in 2013). The study was approved by ethics committee of Xuancheng People's Hospital (No. 2022-LW007-01). Informed consent was taken from all the patients. Anqing Municipal Hospital in Anhui was informed and agreed with the study.

References

1. Liu C, Liu CF, Chen ZH. Research progress on clinical, pathological and molecular diagnosis of pneumonic lung cancer. Chinese Journal of Pulmonary Disease 2018;11:3.
2. Zong Q, Zhu F, Wu S, et al. Advanced pneumonic type of lung adenocarcinoma: survival predictors and treatment efficacy of the tumor. Tumori 2021;107:216-25.
3. Li Q, Fan X, Huo JW, et al. Differential diagnosis of localized pneumonic-type lung adenocarcinoma and pulmonary inflammatory lesion. Insights Imaging 2022;13:49.
4. Huo JW, Huang XT, Li X, et al. Pneumonic-type lung adenocarcinoma with different ranges exhibiting different clinical, imaging, and pathological characteristics. Insights Imaging 2021;12:169.
5. Kim TH, Kim SJ, Ryu YH, et al. Differential CT features of infectious pneumonia versus bronchioloalveolar carcinoma (BAC) mimicking pneumonia. Eur Radiol 2006;16:1763-8.
6. Liu J, Shen J, Yang C, et al. High incidence of EGFR mutations in pneumonic-type non-small cell lung cancer. Medicine (Baltimore) 2015;94:e540.
7. Chen BY, Guan YB, Li JX, et al. CT manifestations and pathological features of pneumonia-type lung cancer. Chinese Journal of Medical Imaging 2013;21:4.
8. Chu ZG, Sheng B, Liu MQ, et al. Differential Diagnosis of Solitary Pulmonary Inflammatory Lesions and Peripheral Lung Cancers with Contrast-enhanced Computed Tomography. Clinics (Sao Paulo) 2016;71:555-61.
9. Gazdar AF, Minna JD. Cigarettes, sex, and lung adenocarcinoma. J Natl Cancer Inst 1997;89:1563-5.
10. Wang BY, Huang JY, Chen HC, et al. The comparison between adenocarcinoma and squamous cell carcinoma in lung cancer patients. J Cancer Res Clin Oncol 2020;146:43-52.
11. Lederlin M, Puderbach M, Muley T, et al. Correlation of radio- and histomorphological pattern of pulmonary adenocarcinoma. Eur Respir J 2013;41:943-51.
12. Ma CH, He XQ, Chen HY, et al. Clinical and ct features of lobar pneumonia and pneumonia lung cancer localized to a single lobe. Journal of Chongqing Medical University 2020;45:4.
13. Cai CY, Gu H, He GY, et al. The diagnostic value of MSCT for lung cancer with peripheral ground-glass opacity. Journal of Practical Radiology 2018;34:4.
14. Travis WD, Brambilla E, Noguchi M, et al. International associa ion for the study of lung cancer/American thoracic society/Europeanrespiratory society international multidisciplinary classification of lung adenocarcinoma. Thorac Oncol 2011;6:244285.
15. Lantuejoul S, Rouquette I, Brambilla E, et al. New WHO

classification of lung adenocarcinoma and preneoplasia. Ann Pathol 2016;36:5-14.
16. Mo XJ, Du FZ, Wang P, et al. CT imaging findings of pneumonia-type lung adenocarcinoma. Medical Imaging Journal 2021;31:5.
17. Hu BH, Chen CZ. Recommended Scheme of Grading Imaging Examination of Ten Malignant Tumors (Version 1.0) for Lung Cancer. Chinese Journal of Medical Computer Imaging 2019;25:427-33.
18. Cohen JG, Reymond E, Jankowski A, et al. Lung adenocarcinomas: correlation of computed tomography and pathology findings. Diagn Interv Imaging 2016;97:955-63.
19. Cao WB, Luo W, Yuan W, et al. The diagnostic value of 128-slice CT volume scan three-dimensional reconstruction combined with dual-phase enhancement for early peripheral small lung cancer. Journal of Practical Radiology 2019;35:4.
20. Isaacs H Jr. Fetal and neonatal cardiac tumors. Pediatr Cardiol 2004;25:252-73

Cite this article as: Xiang Y, Zhang M, Zhao W, Shi H. Differentiation of localized pneumonic-type lung adenocarcinoma from localized pulmonary inflammatory lesion based on clinical data and multi-slice spiral computed tomography imaging features. Transl Cancer Res 2023;12(1): 113-124. doi: 10.21037/tcr-22-2525

